



Article

Effect of Molecular Weight of Tilapia (*Oreochromis Niloticus*) Skin Collagen Peptide Fractions on Zinc-Chelating Capacity and Bioaccessibility of the Zinc-Peptide Fractions Complexes in Vitro Digestion

Lei Chen ^{1,2} , Xuanri Shen ^{1,2,3,*} and Guanghua Xia ^{1,2,3,*} 

¹ Hainan Engineering Research Center of Aquatic Resources Efficient Utilization in South China Sea, Hainan University, Haikou 570228, Hainan, China; chenlei24303@163.com

² College of Food Science and Technology, Hainan University, Haikou 570228, Hainan, China

³ Collaborative Innovation Center of Seafood Deep Processing, Dalian Polytechnic University, Dalian 116000, Liaoning, China

* Correspondence: xuanrishen@hainu.edu.cn (X.S.); 993050@hainu.edu.cn (G.X.); Tel.: +135-1889-8909 (X.S.)

Received: 19 February 2020; Accepted: 12 March 2020; Published: 17 March 2020



Featured Application: The work can provide a certain theoretical basis for the production and preparation of zinc supplement and improve the added value of tilapia skin.

Abstract: To investigate the effect of the molecular weight of tilapia skin collagen peptide fractions on their zinc chelation capacity and the bioaccessibility of their zinc complexes, we evaluated the zinc-chelating ability of different molecular weight peptide, the solubility, and the stability of the complexes during simulated in vitro digestion. Low molecular weight peptide (P1) exhibited a higher zinc-chelating ability, which can be attributed to the variety of metal chelate amino acid residues. The highest solubility and the lowest release of zinc during peptic digestion for the P1-zinc complex and the zinc binding to P1 were retained at approximately 50% after peptic-pancreatic digestion. Fourier transform infrared spectroscopy indicated the primary involvement of the N-H group in all peptide-zinc complexes. This finding suggests that low molecular weight peptide fraction with strong zinc chelation ability can be used as delivery agents to improve zinc bioaccessibility.

Keywords: collagen peptide fractions; molecular weight; zinc; bioaccessibility; surface charge

1. Introduction

Zinc, as an essential micronutrient, is critical to human health and involved in several biological processes, such as enzyme catalysis, DNA replication, RNA transcription, cellular signal transduction, and carbohydrate metabolism [1]. Zinc also plays significant roles in regulating cell growth, gene expression, and immune responses [2]. Non-digestible plant components as diverse as phytate and fiber can bind with zinc to form insoluble complexes, which can restrain zinc absorption in an organism, and calcium ions, high concentrations of ferrous ions, and folic acid are also perceived to inhibit zinc absorption during gastrointestinal tract digestion, thereby leading to zinc deficiency [1–3]. Symptoms of zinc deficiency, including growth defects, gonadal dysfunction, dermal and immune alterations, and neurological dysfunctions [4,5] are widespread in developing countries. Because of its low bioavailability and its ability to cause gastrointestinal tract irritation after long-term consumption [6], the use of zinc salt as a general source of zinc supplement has decreased. Accordingly, it is particularly important to determine alternative methods to enhance the absorption and the bioaccessibility of zinc.

Research on food-derived nutritional supplements has significantly risen in recent years. Compared with zinc salt and zinc-protein complexes, food-derived chelating peptides possess metal ligands such as His, Cys, Asp, Glu, and Ser, which can bind with zinc to form soluble complexes with higher dietary zinc absorption and bioaccessibility [2,7,8]. For example, the solubility of the oyster protein hydrolysate-zinc complex is markedly increased compared with that of ZnSO₄ in various buffer solutions and simulated gastrointestinal digestion conditions, which indicates that this protein hydrolysate-zinc complex can enhance zinc bioaccessibility [9]. Whey-derived peptides with high-magnitude net negative surface charge have strong zinc chelation capacity with high gastric stability, which can enhance zinc delivery. However, their zinc bioaccessibility is reduced during gastrointestinal (GI) digestion. The stability of the peptide-zinc complex affects the release of zinc during gastric digestion, and zinc ion could combine with phytic acid upon entering the duodenum, thereby inhibiting zinc absorption and bioaccessibility [10].

The structural properties of peptides, such as their molecular weight and amino acid residues, are related to their metal-chelating activity, which can affect the bioaccessibility of the metal. A previous study confirmed that the contents of His, Glu, Cys, and Asp in peptides contribute to the metal-chelating activity [11]. The molecular weight of the peptide also influences the metal-chelating activity. However, many studies have reported that both low molecular weight peptides and high molecular weight peptides exhibit higher metal-chelating activity [12,13]. These inconsistent results are still not completely understood.

One of the largest freshwater cultured fish in China is tilapia. The processing utilization rate is only 30–40%, and a massive amount of non-edible by-product, including fish skin, a potential source of collagen, is produced. The use of tilapia skin-derived collagen poses no risk of disease transmission and faces no religious barriers, and this high-yield product can serve as an excellent substrate for the production of peptides [14]. Many studies have focused on the purification of metal-chelating collagen peptides and the preparation and analysis of peptide-zinc complexes [9,11,15]. However, there is little information on the relationship between the molecular weight and zinc-chelating activity of collagen peptide fractions. Therefore, this study aimed to investigate the role of the molecular weight of collagen peptide fractions in their zinc chelation capacity and the zinc solubility. Furthermore, the stability and zinc bioaccessibility of their zinc complexes *in vitro* were also assessed.

2. Materials and Methods

2.1. Materials

Different tilapia skin collagen peptide fractions (P1, P2, and P3) were provided by Hainan Shengmeino Biotechnology Co., Ltd. Pepsin and pancreatin were purchased from Sigma-Aldrich Inc. (Sigma-Aldrich Co., St. Louis, MO, USA). Zinc lactate was purchased from Shanghai Quanwang Biotechnology Co., Ltd. All other reagents used in this study were analytical grade.

2.2. Determination of Molecular Weight of Peptide Fractions

The samples were determined by using a high-performance liquid chromatography system (Daojing Ltd., Tokyo, Japan) on a TSK -GEL G2000 SWXL column (Tosoh Ltd., Tokyo, Japan) [14]. The samples (5 mg/mL) were eluted using an isocratic gradient of 0.1 mol/L PBS with 0.1 mol/L Na₂SO₄ (pH 6.7) at a flow rate of 0.5 mL/min and was monitored at 214 nm. Loading quantity of sample was 20 µL. Molecular weight standards were VB₁₂ (1355 Da), cytochrome C (12,384 Da), trasyolol (6,511 Da), bacitracin (1,450 Da), glutathiol (512.63 Da), Gly-Gly-Tyr-Arg (451 Da), Gly-Gly-Gly (189 Da).

2.3. Preparation of the Peptide Fractions-Zinc Complexes

The peptide fractions-zinc complexes were prepared following the method described by Udechukwu, Downey, and Udenigwe [10] with some modifications. The peptide fraction (10 mg/mL) was dissolved in 50 mM phosphate buffer (pH 6.0) containing 5 mmol/L zinc lactate. The reaction

was carried out at room temperature for 40 min under stirring. After incubation, the free zinc was removed by dialysis for 5 h using a <500 Da molecular weight cut-off semipermeable membrane, and the retentates were freeze-dried to obtain the intact chelate powders.

2.4. Determination of Zinc Chelating Ability

The zinc-chelating ability was determined according to the method described in the literature with some modifications [15]. The zinc content in the complexes, as mentioned above, was determined by atomic absorption spectrometry (Beijing general instrument co., ltd., Beijing, China). The following formula was used to calculate the zinc-chelating ability:

$$\text{Zinc chelating ability} = \frac{\text{Zinc content in complex}}{\text{Total zinc content}} \times 100\%$$

2.5. Determination of Zeta Potential of Peptide

The zeta potential of peptide fractions with different molecular weights was determined using a Zetasizer Nano S90 (Malvern Instruments Ltd., Malvern, UK). The sample was dissolved in deionized water to a final concentration of 1 mg/mL. The solution was contained in a capillary tube after equilibration for 2 min at 25 °C, and then the zeta potential was detected.

2.6. Amino Acid Composition Analysis

Peptide fractions and their zinc complexes were hydrolyzed by 6 M HCl for 24 h at 110 °C and analyzed by HPLC (Agilent 1100 HPLC, Agilent Ltd., USA). The amino acid composition of the sample was calculated as mole%.

2.7. Fourier Transform Infrared (FTIR) Spectroscopy

Peptide fractions and peptide fractions-zinc complexes were qualitatively analyzed using a FTIR spectrometer (Bruker ltd., Massachusetts, USA). Sample preparation was carried out as follows. First, trace samples and 20 mg KBr were mixed in an agate mortar, fully ground under drying conditions. Second, the mixture was ground into a fine powder and used to make the transparent KBr piece. The spectra were recorded at a resolution of 2 cm⁻¹ in the range of 4000 cm⁻¹ to 400 cm⁻¹, with an average of 32 scans.

2.8. Zinc Solubility in Various pH Values

The solubility of the peptide fractions-zinc complexes was determined according to the literature with some modifications [16]. Diverse pH conditions were generated using appropriate buffers at 0.1 mol/L (KCl-HCl and citric acid phosphate buffer solution). The zinc-peptide fractions complexes were dissolved in the solution mentioned above to a final concentration of 1 mg/mL. After shaking at 37 °C for 2 h, the samples were centrifuged at 2500 g for 20 min at 20 °C, and the supernatant was collected. The content of zinc was determined by atomic absorption spectrometry (TAS-990 Super AFG). The zinc solubility was calculated as follows:

$$\text{zinc solubility} = \frac{\text{zinc in supernatant}}{\text{total zinc in solution}} \times 100\%$$

2.9. Determination of Zinc Dialyzability and Stability Under Simulated Gastrointestinal Digestion

Zinc dialyzability was determined using the method described in the literature with some modifications [8,10]. The peptide fractions-zinc complexes dispersed in deionized water to a final concentration of 1 mg/mL were pre-incubated at 37 °C for 30 min. The mixtures were maintained to pH 2.0 before pepsin (1:100, w/w) was added. The solutions were incubated at 37 °C for 1 h and stirred continuously, followed by dialysis to remove free zinc. Next, a portion of the retentate was

freeze-dried to determine the gastric stability of the complex. The other part was adjusted to pH 7.5 with 1 mol/L NaOH and kept pH stability during the simulated intestinal digestion. Pancreatin was added to the above solution, followed by continuous incubation at 37 °C for 3 h. Then, the mixture was dialyzed, and the retentates were freeze-dried to obtain powder. Peptide fraction were used as controls. The zinc content of the three peptide fractions-zinc complexes and their peptic and peptic-pancreatic digests were analyzed by atomic absorption spectrometry (TAS-990 Super AFG). The gastric stability was calculated from the amount (%) of zinc released after pepsin hydrolysis. Zinc dialyzability (bioaccessibility) was calculated using the following formula:

$$\text{Zinc dialyzability} = \frac{\text{total amount of dialyzed Zn}}{\text{Zn in pepsin digest}} \times 100\%$$

2.10. Statistical Analysis

Statistical analysis was conducted by using SPSS software (SPSS Inc., Chicago, USA) for one-way ANOVA and multiple comparisons. All experiments were carried out in triplicate and data were presented as the means \pm standard deviations of various samples. Statistical significances ($p < 0.05$) were evaluated by LSD test.

3. Results and Discussion

3.1. The Molecular Weight Distribution of Peptide Fractions

The distributions of different peptide fractions with molecular weight were shown in Table 1. The components of the peptides were divided into three groups (<1000 Da, 1000–3000 Da, and >3000 Da). The average molecular weight of the samples was 1653 Da (P1), 2745 Da (P2), and 4378 Da (P3), respectively.

Table 1. Molecular weight distribution of peptide fractions.

Molecular Weight Range	Percentage of Peak Area (%)		
	P1	P2	P3
>3000 Da	15.19	32.52	52.38
1000–3000 Da	39.14	32.30	30.66
<1000 Da	45.67	35.18	16.96
Average molecular weight (AMW)/Da	1653	2745	4378

3.2. Zinc-Chelating Capacity of the Peptide

Different molecular weight hydrolysate fractions had different physicochemical properties and functional properties [17]. Figure 1 presents the zinc chelation capacity of the peptide fractions. The zinc chelation capacity decreased from $33.25 \pm 1.03\%$ to $19.44 \pm 0.89\%$, as the molecular weight of the peptide fractions increased. The zinc chelation capacity of P1 with higher surface charge, was higher than that of the other two groups. A peptide fraction with higher potential has more negative surface charges, which may provide more zinc-binding sites. It was apparent that the higher potential of peptide which can attract more zinc ions chelate to the anionic surface of the peptide fraction, although they exhibit similar amino acid composition. Furthermore, the molecular weight of peptide fractions is proportional to their dispersion, surface hydrophobicity, and particle size [18–20]. Zhang suggested that the low molecular weight pig skin collagen peptides with higher degree of hydrolysis exhibited higher surface hydrophobicity and charge, which have better stability and dispersion in solution. [21]. These results suggest that the molecular weight can be used as an indicator to predict the zinc chelation capacity pattern of a peptide. Fish collagen peptides have been reported to bind with several metals, such as Fe, Cu, and Ca [11]; however, this study is the first to report their zinc chelation capacity and the influence of molecular weight on the zinc chelation capacity.

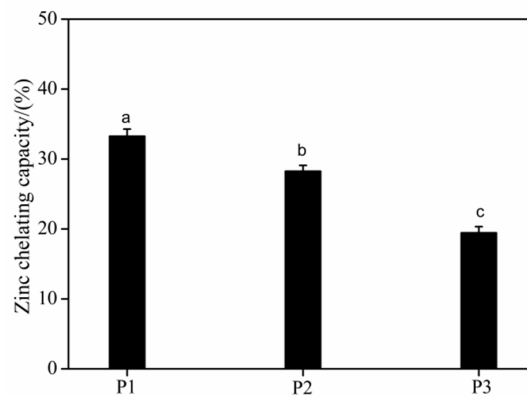


Figure 1. Zinc chelating capacity of three molecular weight peptide fractions; bars in each chart with different letters represent significantly different mean values with $P < 0.05$.

3.3. Zeta Potential of the Peptide Fractions

The net negative charge of each peptide fraction was determined from its zeta potential and the value of zeta potential determined surface phenomena occurring at the interface. The zeta potential values of the three peptide fractions of different molecular weights are presented in Figure 2. There was a clear trend of the potential increasing from -12.91 ± 2.04 mV for P1 to -5.83 ± 0.97 mV for P3. As the molecular weight of the peptide fraction increased, the absolute value of the zeta potential decreased. This can be attributed to the changes in the surface charge distribution of the native protein on the basis of its molecular rearrangement during hydrolysis and the repulsive intermolecular electrostatic force increased with the increase in the degree of hydrolysis (DH). Furthermore, the molecular weight of hydrolysate fraction decreases with the increase of DH under certain hydrolysis conditions and it indicated that low molecular weight peptide fraction with higher DH exhibited the higher surface charge. The surface charge of the peptides was conducive to the stability of the particles except when the particle size could not be balanced with electrostatic repulsion [16,21,22]. The low molecular weight peptide fraction P1 exhibited the strong zinc chelation capacity, this can be due to the high electrostatic repulsion at P1 surface, reflected by high magnitude zeta potential, which inhibit intermolecular aggregation leading to small peptide particles. The iron chelation capacity of sea cucumber ovum hydrolysates, as well as the stability of their iron complexes, was influenced by their net negative charge [23]. The zeta potential of the peptides indicated that they possessed different degrees of stability in aqueous solution, which affected their affinity for metal ions and the stability of their metal complexes [24]. The low molecular weight of peptide fraction with higher surface charge is considered to be related to the strong zinc chelation capacity and stability of the zinc-peptide complexes.

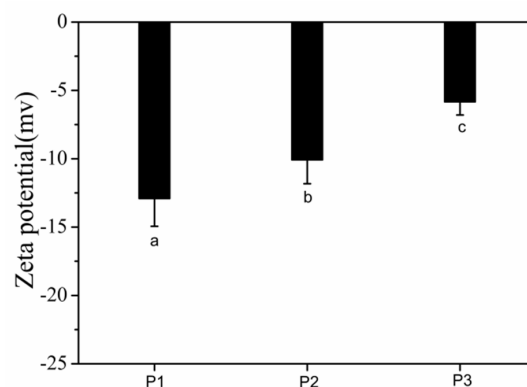


Figure 2. Zeta potential of three molecular weight peptide fractions; bars in each chart with different letters represent significantly different mean values with $P < 0.05$.

3.4. Amino Acid Composition

The functions of the peptide are determined by the amino acid composition. The amino acid composition of peptide fractions was shown in Table 2. The hydrophilic amino acids including aspartic acid (Asp), arginine (Arg), and histidine (His) were correlated with metal-binding activities [23] and there was no significant difference on the contents of amino acids in different molecular weight peptides fractions. However, we found that Asp residue of three peptide fractions all did not participate in the reaction, particularly. Furthermore, the contents of other hydrophilic amino acids (Arg and His) in P3 had decreased after chelating with zinc.

Table 2. Amino acid composition (mole/%) of three molecular weight peptide fractions and their zinc complexes.

Amino Acid	P1	P1-Zn	P2	P2-Zn	P3	P3-Zn
Glu	7.76	7.80	7.82	7.63	7.91	7.61
Ser	3.17	3.21	3.17	3.17	3.22	3.07
His	0.53	0.55	0.53	0.56	0.52	0.49
Gly	40.50	40.61	41.06	39.51	41.25	39.62
Thr	2.48	2.57	2.52	2.51	2.57	2.46
Arg	5.05	5.12	5.23	5.09	5.15	4.89
Ala	13.75	13.76	13.86	13.57	13.92	13.38
Tyr	0.23	0.17	0.15	0.14	0.17	0.13
Cys	1.52	1.64	1.44	2.31	1.63	1.57
Val	1.93	1.97	1.92	1.94	1.98	1.90
Met	1.00	0.87	0.75	0.94	0.80	0.81
Phe	1.26	1.26	1.25	1.24	1.27	1.22
Ile	0.96	0.96	0.95	0.95	0.96	0.93
Leu	2.17	2.17	2.17	2.16	2.19	2.11
Lys	2.62	2.67	2.71	2.56	2.73	2.60
Pro	10.39	10.05	9.82	11.13	9.02	12.67
Asp	4.66	4.65	4.66	4.61	4.71	4.54

Compared with high molecular weight peptide fraction P3, various of amino acids in low molecular weight peptide fraction P1 with strong zinc chelating capacity participated in zinc chelation reaction except the hydrophilic amino acids. Additionally, the acidic-amino acids (His and Cys), serine (Ser), and glycine (Gly) in P1 were involved in the chelating reaction, but the contents of those amino acids had decreased in P3 after binding with zinc. This can be attribute to the low molecular weight peptide with higher surface charge, which provide more sites for chelating zinc and the occurrence of higher DH lead to the exposure of more amino acid residues whose side chains can participate in zinc coordination [10,21]. A study of chelating peptides from oyster protein hydrolysates indicated that acidic amino acid residues including His and Cys were the major binding sites of zinc ion [15]. Guo et al. [11] reported that Ser residues played an important role in the metal chelation reaction. Wang et al. [25] reported that Gly can participate in the formation of complex Al(III). In addition, the imidazole ring of His and thiolate group of Cys in low molecular weight peptide fraction was able to efficiently chelate metal ions [26]. Metal ions could simultaneous bound with more bind sites including the N-terminal amino group and a distant donor atom in a macrochelate structure which caused by the presence of Pro in the internal position of the peptide sequence [26,27], and the content of Pro with metal chelation capacity in P2 and P3 was remarkably lower than P1, but participated in the reaction. A previous study found that the combination of high His content and small peptide size was correlated with high copper chelating activity [28]. This result suggests that a variety of amino acids in low weight molecular peptide fraction with strong zinc chelation capacity involve in the chelation than in high molecular weight peptide fraction and it can provide more site for bounding zinc to forming a stable complex.

3.5. Characterization of the Zinc-Peptide Fractions Interactions by FTIR

The functional groups related to the chelate of zinc in the peptide fractions-zinc complexes were investigated by infrared spectroscopy [29]. There were no significant differences in the infrared spectra of the three peptide fractions or their zinc complexes, which indicated that these peptide fractions with different molecular weights have similar zinc-binding ligands in nature. The wavenumbers of the notable band shifts in the infrared spectra of these samples are listed in Table 3. There is a significant difference in the spectral band position and intensity between the peptide fractions and their peptide-zinc complexes. The characteristic absorption band of amide A is between 3300 cm^{-1} and 3440 cm^{-1} and is mainly related to N-H stretching [30]. The wavenumbers of the amide A band were 3316 , 3388 , and 3419 cm^{-1} for the three peptide fractions and distinctly shifted to 3403 , 3415 , and 3426 cm^{-1} , respectively, for the three peptide-zinc complexes. This shift may be due to the electron-withdrawing effect of Zn^{2+} and the nitrogen atoms can form coordination bonds with zinc ions by offering their electron pairs, the hydrogen bonds were replaced with Zn-N bonds [31,32]. Compared with the other two peptide fractions, P3 exhibited less N-H stretching, which suggested that P3 had a weaker affinity for Zn^{2+} .

Table 3. Wavenumber (cm^{-1}) of band shifts observed in the FTIR spectra of three molecular weight peptide fractions and their zinc complexes.

Functional Groups	P1	P1-Zn	P2	P2-Zn	P3	P3-Zn
N-H	3316	3403	3388	3415	3419	3426
Amide I	1651	1650	1651	1652	1652	1647
Amide II	1542	1546	1542	1545	1541	1545
COO-	1400	1402	1399	1402	1401	1403
Amide III	1334	1336	1334	1337	1334	1337
Amide VI	658	591	659	570	659	597

The absorption band of the peptide fractions in the range of $1600\text{--}1700\text{ cm}^{-1}$, characterized as the amide I band, was attributed to the C=O stretching vibrations coupled with the bending vibrations of N-H. There was no remarkable shift in this band for the peptide-zinc complexes, which indicated that the C=O of the peptide fractions was not intimately coordinated with Zn^{2+} . Amide II bands ($1500\text{--}1600\text{ cm}^{-1}$), caused by N-H bending coupled with C-N stretching, shifted slightly with the different molecular weight of the peptide fractions [33]. The peak corresponding to the -COO^- carboxylate group was different for any of the Zn^{2+} -treated peptide fractions, which may result from the replacement of H with zinc. The positions of the bands for amide III (Barth, 2007), caused by both N-H in-plane bending and C-N stretching vibrations, shifted slightly in the spectra of three chelates. The peak at 658 cm^{-1} , caused by the completely in-plane vibration of the O=C-N bond was shifted to 591 (P1-Zn), 570 (P2-Zn), and 597 cm^{-1} (P3-Zn) when peptide fractions were bound to zinc, which was caused by the increasing electron cloud density of $\text{O}=\text{CH}_2$ and decreasing electron cloud density of N-H, shifted [34,35]. The FTIR results suggest that some functional peptide groups were more or less involved in Zn^{2+} binding, the amino group was the primary Zn^{2+} reaction site in the low molecular weight collagen peptide fraction.

3.6. Zinc Solubility at Various pH Values

Zinc solubility is one of the significant components that can affect zinc absorption and availability [16]. Figure 3 presents the experimental data on the zinc solubility of the three peptide fractions-zinc complexes at various pH values. The three peptide-zinc complexes exhibited higher zinc-releasing capacity at pH 2–6. Higher solubility of metal ions in acidic pH increases their absorption in the duodenum and proximal jejunum. When the pH was increased to 7 and 8, the amount of zinc released was dramatically diminished, and the zinc absorption rate was markedly reduced in the distal small intestine. In weakly alkaline conditions, a portion of Zn^{2+} could combine with -OH to form

precipitates [15], which decreases the zinc content in the supernatant. The pH in the human intestinal tract is approximately 7.2, and the P1-Zn complex exhibited higher zinc solubility in the weakly basic conditions, potentially because low molecular weight peptide fraction with highly exposed side chains and higher surface charges provide more binding sites for peptide-zinc complexes formation, which could decrease zinc precipitation and interactions with other metals [36]. Furthermore, zinc, which chelates amino acids and loosely binds to intracellular proteins, is the available forms of zinc mineral inside enterocytes or intestinal absorptive cells. Therefore, P1 has higher zinc chelation capacity than other peptide fractions and can enhance the solubility of zinc at neutral pH conditions.

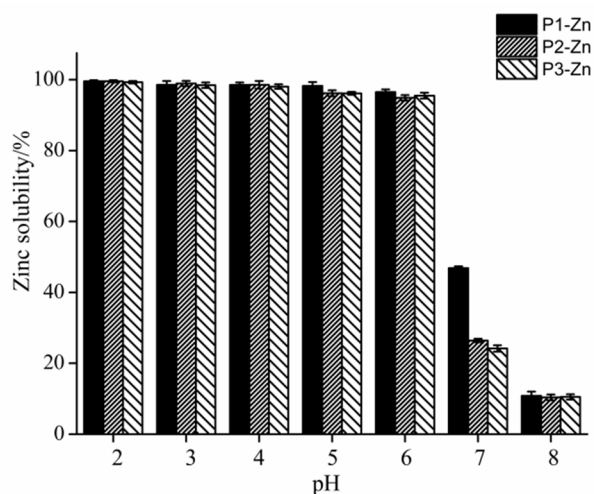


Figure 3. Zinc solubility of three peptide-zinc complexes at various pH values.

3.7. Gastric Stability and Zinc Dialyzability

The structural properties, such as the molecular weight and amino acid composition, of peptides can influence the behavior of their metal complexes. Zinc release is attributed to the disintegration of the complex at the acidic gastric pH and the proteolytic action of pepsin, which causes further hydrolysis of peptide and dissociation of their zinc complexes [10]. Unsurprisingly, zinc was released from the three peptide fractions-zinc complexes during simulated gastrointestinal digestion. However, zinc release was notably lower from the P1-zinc complex than from the other complexes (Table 4), which indicated that a peptide fraction-zinc complex with low molecular weight was more stable in the gastric phase, possibly because of its high net negative surface charge [37]. Zinc release from the three peptide-zinc complexes significantly increased after further digestion by pancreatin but remained highest for P1-zinc than for the others (Table 3). A similar study found that two whey protein-derived peptide-zinc complexes with different chelation capacities released low amounts of zinc during simulated gastric digestion but released large quantities of zinc after hydrolysis by pancreatic enzymes [10]. Peptide fractions with a net charge are expected to maintain their zinc chelation capacity at pancreatic pH. Therefore, the release of zinc at this pH can be attributed to further cleavage by pancreatic enzymes, which is desirable for intestinal absorption. The C-terminal end of both Cys and Ser can be hydrolyzed by pancreatic enzymes, while the contents of Cys and Ser in the P1-Zn complex was higher than that in the other complexes and could lead to higher hydrolysis [38]. As a result, zinc dialyzability is higher for low molecular weight peptide fraction-zinc complex, with higher solubility, than for high molecular weight peptide fraction, indicating that the zinc delivered via the former is more bioaccessible (available for absorption). However, more than half of the zinc was retained in the three peptide-zinc complexes after simulated gastric intestinal digestion. The molecular weight of peptide fraction can influence the formation and stability of the zinc complexes, which indicated that peptide structure can affect the zinc release from peptide-zinc complexes for intestinal absorption. This

suggest the low molecular weight peptide fraction-zinc complex may have the potential to improve zinc bioavailability and to be used as an ingredient in foods.

Table 4. Zinc release and dialyzability of peptide-zinc complexes after simulated gastric and gastrointestinal digestion of three molecular weight peptide fractions.

Samples	Zinc Released after Peptic Digestion (%)	Zinc Released after Peptic-Pancreatic Digestion (%)	Zinc Dialyzability (Bioaccessibility) (%)
P1	10.29 ± 1.54 ^a	44.05 ± 1.01 ^c	54.34 ± 2.55 ^b
P2	13.41 ± 0.92 ^c	31.94 ± 0.27 ^b	45.35 ± 1.19 ^c
P3	12.11 ± 0.9 ^b	21.12 ± 0.19 ^a	33.23 ± 1.17 ^a

The numbers in each column of different superscript letters represent significantly different averages.

4. Conclusions

This study investigated the zinc chelation capacity of collagen peptide fractions from tilapia skin with different molecular weights and the bioaccessibility of their zinc complexes. The results showed that the low molecular weight peptide fraction P1 with diverse metal-chelating amino acid residues participated in the chelation, exhibited stronger zinc chelation capacity than P3. The FTIR spectra of the three peptide-zinc complexes with different characteristics showed the amino group was the main metal-chelating ligands. Compared to the other two complexes, the P1-zinc complex possessed higher zinc solubility under neutral pH conditions, stronger gastric stability and zinc dialyzability during gastrointestinal digestion. High molecular weight peptide fraction can limit zinc dialyzability from complexes, which can influence zinc bioaccessibility, and this effect was more pronounced in the P3-zinc complex. Therefore, peptide fractions with low molecular weight can improve gastric stability and zinc absorption during intestinal digestion. In *in vivo* studies focusing on determining their bioaccessibility of zinc in complexes with low molecular weight peptide fractions and their practical ability to enhance zinc absorption will be further carried out.

Author Contributions: Conceptualization, L.C.; Data curation, L.C.; Formal analysis, L.C.; Funding acquisition, X.S.; Investigation, L.C.; Methodology, L.C.; Project administration, X.S.; Software, L.C.; Supervision, X.S. and G.X.; Validation, L.C.; Visualization, L.C.; Writing—original draft, L.C.; Writing—review & editing, L.C. and G.X. All authors have read and agreed to the published version of the manuscript.

Funding: This research was funded by National Key R&D Program of China, grant number 2018YFD0901103; Marine and Fisheries Bureau of Haikou, grant number HHCL201804; Scientific Research Foundation of Hainan University, grant number KYQD1662.

Acknowledgments: This work was supported by the funding of the National Key R&D Program of China [No. 2018YFD0901103]; the Marine and Fisheries Bureau of Haikou [No. HHCL201804]; and the Scientific Research Foundation of Hainan University [No. KYQD1662].

Conflicts of Interest: We declare that there are no conflicts of interest.

References

- Nriagu, J. Zinc deficiency in human health. *Encycl. Environ. Health* **2011**, 789–800.
- Udechukwu, M.C.; Collins, S.A.; Udenigwe, C.C. Prospects of enhancing dietary zinc bioavailability with food-derived zinc-chelating peptides. *Food Funct.* **2016**, *7*, 4137–4144. [[CrossRef](#)] [[PubMed](#)]
- Hambidge, M. Human zinc deficiency. *J. Nutr.* **2000**, *130*, 1344–1349. [[CrossRef](#)] [[PubMed](#)]
- Prasad, A.S. Discovery of human zinc deficiency: 50 years later. *J. Trace Elem. Med. Biol.* **2012**, *26*, 66–69. [[CrossRef](#)] [[PubMed](#)]
- Bonaventura, P.; Benedetti, G.; Albarède, F.; Miossec, P. Zinc and its role in immunity and inflammation. *Autoimmun. Rev.* **2015**, *14*, 277–285. [[CrossRef](#)]

6. Akbar, B.; Niloufar, N.; Abolfazl, M.; Lofollah, S.; Ali, K.Q.; Soheyla, V. Evaluation and comparison of zinc absorption level from 2-alkyle 3-hydroxy pyranonzinc complexes and zinc sulfate in rat in vivo. *Adv. Biomed. Res.* **2013**, *2*, 77–80. [[CrossRef](#)]
7. Guo, L.; Harnedy, P.A.; Li, B.; Hou, H.; Zhang, Z.; Zhao, X. Food protein-derived chelating peptides: Biofunctional ingredients for dietary mineral bioavailability enhancement. *Trends Food Sci. Technol.* **2014**, *37*, 92–105. [[CrossRef](#)]
8. Wang, X.; Zhou, J.; Tong, P.; Mao, X. Zinc-binding capacity of yak casein hydrolysate and the zinc-releasing characteristics of casein hydrolysate-zinc complexes. *J. Dairy Sci.* **2011**, *94*, 2731–2740. [[CrossRef](#)]
9. Chen, D.; Liu, Z.; Huang, W.; Zhao, Y.; Dong, S.; Zeng, M. Purification and characterization of a zinc-binding peptide from oyster protein hydrolysate. *J. Funct. Foods* **2013**, *5*, 689–697. [[CrossRef](#)]
10. Udechukwu, M.C.; Downey, B.; Udenigwe, C.C. Influence of structural and surface properties of whey-derived peptides on zinc-chelating capacity, and in vitro gastric stability and bioaccessibility of the zinc-peptide complexes. *Food Chem.* **2018**, *240*, 1227–1232. [[CrossRef](#)]
11. Guo, L.; Harnedy, P.A.; O’Keeffe, M.B.; Zhang, L.; Li, B.; Hou, H. Fractionation and identification of alaska pollock skin collagen-derived mineral chelating peptides. *Food Chem.* **2015**, *173*, 536–542. [[CrossRef](#)] [[PubMed](#)]
12. Lv, Y.; Bao, X.L.; Yang, B.C.; Ren, C.G.; Guo, S.T. Effect of soluble soybean protein hydrolysate-calcium complexes on calcium uptake by Caco-2 cells. *J. Food Sci.* **2008**, *73*, 1750–3841. [[CrossRef](#)] [[PubMed](#)]
13. Wang, C.; Li, B.; Ao, J. Separation and identification of zinc-chelating peptides from sesame protein hydrolysate using IMAC-Zn²⁺ and LC-MS/MS. *Food Chem.* **2012**, *134*, 1231–1238. [[CrossRef](#)] [[PubMed](#)]
14. Mei, F.-F.; Liu, J.-J.; Wu, J.-T.; Duan, Z.-W.; Meng, K.-K.; Chen, S.-J.; Shen, X.-R.; Xia, G.-H.; Zhao, M.-H. Collagen peptides isolated from salmo salar and tilapia nilotica skin accelerate wound healing by altering cutaneous microbiome colonization via upregulated NOD2 and BD14. *J. Agric. Food Chem.* **2020**, *68*, 1621–1633. [[CrossRef](#)]
15. Zhang, Z.; Zhou, F.; Liu, X.; Zhao, M. Particulate nanocomposite from oyster (*Crassostrea rivularis*) hydrolysates via zinc chelation improves zinc solubility and peptide activity. *Food Chem.* **2018**, *258*, 269–277. [[CrossRef](#)]
16. Eckert, E.; Bamdad, F.; Chen, L. Metal solubility enhancing peptides derived from barley protein. *Food Chem.* **2014**, *159*, 498–506. [[CrossRef](#)]
17. Pagán, J.; Ibarz, A.; Falguera, V.; Benítez, R. Enzymatic hydrolysis kinetics and nitrogen recovery in the protein hydrolysate production from pig bones. *J. Food Eng.* **2013**, *119*, 655–659. [[CrossRef](#)]
18. Li, Z.-R.; Wang, B.; Chi, C.-F.; Gong, Y.-D.; Luo, H.-Y.; Ding, G.-F. Influence of average molecular weight on antioxidant and functional properties of cartilage collagen hydrolysates from *Sphyrna lewini*, *Dasyatis akjei* and *Raja porosa*. *Food Res. Int.* **2013**, *51*, 283–293. [[CrossRef](#)]
19. Hera, E.; Gomez, M.; Rosell, C.M. Particle size distribution of rice flour affecting the starch enzymatic hydrolysis and hydration properties. *Carbohydr. Polym.* **2013**, *98*, 421–427. [[CrossRef](#)]
20. Turgeon, S.L.; Gauthier, S.F.; Mollé, D.; Léonil, J. Interfacial properties of tryptic peptides of b-lactoglobulin. *J. Agric. Food Chem.* **1992**, *40*, 669–675. [[CrossRef](#)]
21. Zhang, Y.; Zhang, Y.; Liu, X.; Huang, L.; Chen, Z.; Cheng, J. Influence of hydrolysis behaviour and microfluidisation on the functionality and structural properties of collagen hydrolysates. *Food Chem.* **2017**, *227*, 211–218. [[CrossRef](#)] [[PubMed](#)]
22. Liu, Y.-L.; Li, X.-H.; Chen, Z.-J.; Yu, J.; Wang, F.-X.; Wang, J.-H. Characterization of structural and functional properties of fish protein hydrolysates from surimi processing by-products. *Food Chem.* **2014**, *151*, 459–465. [[CrossRef](#)] [[PubMed](#)]
23. Sun, N.; Cui, P.; Jin, Z.; Wu, H.; Wang, Y.; Lin, S. Contributions of molecular size, charge distribution, and specific amino acids to the iron-binding capacity of sea cucumber (*Stichopus japonicus*) ovum hydrolysates. *Food Chem.* **2017**, *230*, 627–636. [[CrossRef](#)] [[PubMed](#)]
24. Elias, R.J.; Kellerby, S.S.; Decker, E.A. Antioxidant activity of proteins and peptides. *Crit. Rev. Food Sci. Nutr.* **2008**, *48*, 430–441. [[CrossRef](#)]
25. Wang, X.; Li, K.; Yang, X.D.; Wang, L.L.; Shen, R.F. Complexation of Al(III) with reduced glutathione in acidic aqueous solutions. *J. Inorg. Biochem.* **2009**, *103*, 657–665. [[CrossRef](#)]
26. Kozłowski, H.; Kowalik-Jankowska, T.; Jezowska-Bojczuk, M. Chemical and biological aspects of Cu²⁺ interactions with peptides and aminoglycosides. *Coord. Chem. Rev.* **2005**, *249*, 2323–2334. [[CrossRef](#)]

27. Kozłowski, H.; Bal, W. Specific structure-stability relations in metallopeptides. *Coord. Chem. Rev.* **1999**, *184*, 319–346. [[CrossRef](#)]
28. Torres-Fuentes, C.; Alaiz, M.; Vioque, J. Affinity purification and characterisation of chelating peptides from chickpea protein hydrolysates. *Food Chem.* **2011**, *129*, 485–490. [[CrossRef](#)]
29. Reddy, P.; Radhika, M.; Manjula, P. Synthesis and characterization of mixed ligand complex of Zn (II) and Co (II) with amino acids: Relevance to zinc binding sites in zinc fingers. *J. Chem. Sci.* **2005**, *117*, 239–246. [[CrossRef](#)]
30. Liao, W.; Guanghua, X.; Li, Y.; Shen, X.R.; Li, C. Comparison of characteristics and fibril-forming ability of skin collagen from barramundi (*Lates calcarifer*) and tilapia (*Oreochromis niloticus*). *Int. J. Biol. Macromol.* **2017**, *107*, 549–559. [[CrossRef](#)]
31. Qingling, W.; Xiong, Y.L. Zinc-binding behavior of hemp protein hydrolysates: Soluble versus insoluble zinc-peptide complexes. *J. Funct. Foods* **2018**, *49*, 105–112.
32. Van der Ven, C.; Muresan, S.; Gruppen, H.; de Bont, D.B.; Merck, K.B.; Voragen, A.G. FTIR spectra of whey and casein hydrolysates in relation to their functional properties. *J. Agric. Food Chem.* **2002**, *50*, 6943–6950. [[CrossRef](#)] [[PubMed](#)]
33. Curley, D.; Kumosinski, T.; Unrah, J.; Farrell, H. Changes in the secondary structure of bovine casein by fourier transform infrared spectroscopy: Effects of calcium and temperature¹. *J. Dairy Sci.* **1998**, *81*, 3154–3162. [[CrossRef](#)]
34. Fang, Z.; Xu, L.; Lin, Y.; Cai, X.; Wang, S. The preservative potential of octopus scraps peptides–zinc chelate against staphylococcus aureus: Its fabrication, antibacterial activity and action mode. *Food Control* **2018**, *98*, 24–33. [[CrossRef](#)]
35. Barth, A. Infrared spectroscopy of proteins. *Biochim. Biophys. Acta Bioenerg.* **2007**, *1767*, 1073–1101. [[CrossRef](#)] [[PubMed](#)]
36. Miquel, E.; Farré, R. Effects and future trends of casein phosphopeptides on zinc bioavailability. *Trends Food Sci. Technol.* **2007**, *18*, 139–143. [[CrossRef](#)]
37. Chen, M.; Li, B. The effect of molecular weights on the survivability of casein-derived antioxidant peptides after the simulated gastrointestinal digestion. *Innov. Food Sci. Emerg. Technol.* **2012**, *16*, 341–348. [[CrossRef](#)]
38. Wang, C.; Li, B.; Wang, B.; Xie, N. Degradation and antioxidant activities of peptides and zinc-peptide complexes during in vitro gastrointestinal digestion. *Food Chem.* **2015**, *173*, 733–740. [[CrossRef](#)]



© 2020 by the authors. Licensee MDPI, Basel, Switzerland. This article is an open access article distributed under the terms and conditions of the Creative Commons Attribution (CC BY) license (<http://creativecommons.org/licenses/by/4.0/>).